Available online at www.sciencedirect.com
ScienceDirect
Journal of Molecular Catalysis A: Chemical 272 (2007) 298–305
JOURNAL OF MOLECULAR CATALYSIS A: CHEMICAL
www.elsevier.com/locate/molcata

A spectroscopic probe for combined acid and redox properties in acid catalysts

L.M.O.C. Merat [a,b], R.A.S. San Gil [a,*], S.R. Guerra [b], L.C. Dieguez [b], S. Caldarelli [c], J.G. Eon [a], F. Ziarelli [d], Hélène Pizzala [c]

[a] *Instituto de Química, Universidade Federal do Rio de Janeiro, Ed.CT, blocoA/605 Ilha do Fundão C.P.068556, CEP 21941-972 Rio de Janeiro, Brazil*
[b] *NUCAT-PEQ-COPPE, Universidade Federal do Rio de Janeiro, Brazil*
[c] *JE2421 TRACES Université Aix Marseille 13013 Marseille, France*
[d] *Spectropole, Federation des Sciences Chimique FWR1739 1301 Marseille, France*

Received 27 October 2006; received in revised form 15 February 2007; accepted 16 February 2007
Available online 22 February 2007

Abstract

The activity of the catalytic materials used in industrial and academic laboratories often relies on the concurrence of acidic and redox properties. In this work trimethylphosphine was selected as a NMR probe to assess the type and force of a catalyst acid sites as well as an estimate of its redox capabilities by a single set of experiments, since the ^{31}P spectrum of both this molecule and of its oxidized form (TMPO) is sensitive to the solid acidity. The strength of the acidic sites was assessed by the probe chemical shift and its resistance to desorption at high temperature. A qualitative oxidizing scale was evaluated by the facility with which a given solid produces TMPO from TMP. Different catalysts were analysed: γ-Al_2O_3, zeolite HY and K10, KSF and Zr-pillared acid clays. γ-Al_2O_3 was found to form only Lewis adducts and to possess no detectable redox behavior. The zeolite HY tested here had oxidizing properties (probably due to metal or group XVI impurities) and presented adducts with Brönsted as well as with extra-framework aluminum (EFAl) sites. Purely Brönsted sites were observed for K10, KSF and Zr-pillared clays. These latter materials were characterized here for the first time by ^{31}P NMR of adsorbed TMP. ^{31}P MAS NMR spectra of K10 showed three different types of Brönsted sites, but only one seems to be present in the case of KSF and of the Zr-pillared clay.

Keywords: Trimethylphosphine; Trimethylphosphine oxide; ^{31}P MAS NMR; K10 clay; KSF clay; HY zeolite; Zr pillared clay

1. Introduction

The characterization of the Brönsted or Lewis nature of solid acids, as well as the strength and concentration of each active site can help in selecting the appropriate catalyst for a desired application [1]. NMR spectroscopy of phosphorous-containing probe molecules is one of the methods of choice to this respect, because ^{31}P is a nuclide with high relative receptivity (6.6% compared to ^{1}H). Some recent examples of the use of basic phosphine derivatives, and most notably TMP (trimethylphosphine), as a probe for the characterization of the nature of acid sites can be found in the literature [2–4]. In the case of the solids used as actual catalysts, often the presence of impurities contributes to the overall reactivity, adding a redox character to the material. This latter property can be followed by the evolution of the TMP probe into trimethylphosphine oxide (TMPO) [5,6], a molecule that has originally been used to investigate solid acid strength [7]. We set here to investigate the TMP/TMPO system to perform a broad characterization of working catalysts, a task which has not been previously addressed. It is common practice to infer the strength of a given acid site by the chemical shift of probe adduct. Although widely used, this procedure could be misleading, as the resonance position depends on the electron density but on the molecular geometry as well. Therefore we complemented the analysis of the NMR resonance position with a cycle of adsorption followed by desorption under vacuum at high temperature, similarly to common practice for IR spectroscopic probes [8].

In this work we examined three examples of very common solids used in organic synthesis: γ-Al_2O_3 and HY zeolites,

* Corresponding author. Tel.: +55 21 2562 7737; fax: +55 21 2562 7944.
E-mail address: rsangil@iq.ufrj.br (R.A.S.S. Gil).

1381-1169/$ – see front matter © 2007 Elsevier B.V. All rights reserved.
doi:10.1016/j.molcata.2007.02.025

Table 1
Relevant ^{31}P NMR chemical shift values for TMP and TMPO

System	Pure	Physisorbed	Lewis	Brönsted	Reference
TMP	−62	−67	−50	−2 to −6	[19,22,31]
TMPO	39	40–48	53	65–90	[8,14,24]

which are examples of catalysts possessing Lewis [5] and Brönsted [9] acid sites, respectively, and acid clays, for which the nature of the sites is not completely understood and studies are scarce. Clays are used in a number of organic reactions promoted by both Brönsted or Lewis acid sites [10–12].

The interpretation of the ^{31}P NMR data were achieved on the basis of extensive literature work as summarized in Table 1. The influence of the probe molecule on the solid structure has been also followed by ^{27}Al MAS, to distinguish the presence and evolution of low-symmetry sites. This is the case of extraframework aluminum in zeolites [13], which also provides a source of Lewis sites.

2. Experimental

γ-Al_2O_3 was from Engelhard Al-3916P. HY zeolite was from a FCC cracking unit and K10 and KSF were commercial acid clays purchased from Aldrich Co. Zr-pillared clay was prepared from a brazilian montmorillonite from the Bentonit S.A. brazilian montmorillonite (Paraíba, Brazil), with cation exchange capacity (CEC) of 106 mequiv./100 g clay. The clay was dispersed in water, with solid content of 1 g/l, and Zr^{4+} intercalated with 0.1 M zirconium acetate at ambient temperature using an Zr/clay ratio of 10 mmol/g. After treatment the sample was dried at 333 K and calcined at 773 K for 2 h. The solids were characterized by chemical analysis (X-ray fluorescence, Rigaku model RIX-3100 instrument), BET area (Micromeritics ASAP2000 equipment) and pyridine acidity (by FTIR with a Perkin-Elmer 2000 FTIR, self-supporting thin wafers dried at 623 K during 2 h, followed by adsorption of 4 Torr pyridine at 423 K, 4 cm^{-1} resolution, acquisition of 36 scans spectra at ambient temperature and after desorption at 523 and 623 K). The characteristics of the samples are summarized in Table 2.

For the NMR measurements, 60 mg of the sample were introduced into a 4 mm ZrO_2 rotor, which was subsequently transferred to the adsorption cell. The pre-treatment was carried out at 673 K during 2 h for γ-Al_2O_3 and HY and at 623 K during 2 h for K10, KSF and Zr-pillared clay. After adsorption of 40 Torr of TMP at room temperature followed by vacuum application (2×10^{-5} Torr) until no vacuum variation (1–4 h, depending on the sample), the cell was transferred to a glove box and the rotor closed with Kel-F lids under dry nitrogen atmosphere. After the first NMR analysis the rotor returned to the reactor and was evacuated on a Micrometrics ASAP-2010 instrument (2×10^{-5} Torr) at 623 K during 1 h. The rotor was then transferred to a moisture free nitrogen glove box, closed again with a Kel-F cap and maintained in this ambient until the next series of solid-state analysis. NMR spectra were recorded immediately upon adsorption and a month after being transferred to the rotor. The two spectra were identical, so the risk of water contamination of the samples during the experiments was excluded.

^{31}P and ^{27}Al NMR MAS spectra were recorded at 300.13 MHz on a Bruker DRX-300 (7.05 T) spectrometer, operating at 121.4 MHz and 78.2 MHz, respectively, by using a pulse-acquire sequence, at a sample spinning frequency of 6–10 kHz, whereas ^{1}H to ^{31}P CPMAS spectra were acquired on a Bruker DSX-400 MHz (9.4 T) at the frequency of 161.9 MHz. Both instruments used Bruker probes with 4 mm zirconia rotors. All measurements were made at ambient temperature. ^{31}P MAS spectra were obtained by using a $\pi/2$ excitation pulse (7.5 μs) and a recycle time of 30 s. Between 128 and 20k free induction decays were accumulated, depending on the sample studied. ^{27}Al MAS experiments were conducted by using a short $\pi/6$ pulse (1.2 μs) to selectively promote $+1/2 \leftrightarrow -1/2$ transitions, with 3000 scans. ^{1}H–^{31}P CPMAS spectra were obtained with

Table 2
Physicochemical characterization of the solids studied

Catalyst	Chemical analysis[a]	BET area[b] (m^2/g)	Acidity[c] (cm^{-1})
γ-Al_2O_3	Al_2O_3: 98.8%; SiO_2: 0.41%; Fe_2O_3: 0.06%; K_2O: 0.01%; P_2O_5: 0.02%; SO_3: 0.27%; Cl: 0.08%; TiO_2: 0.32%	216	1448, Lewis; vanishes at 623 K
HY zeolite	SiO_2: 70.28%; Al_2O_3: 27.49%; Fe_2O_3: 0.09%; NiO: 0.01%; Na_2O: 0.77%; K_2O: 0.01%; CaO: 0.04%; P_2O_5: 0.22%; SO_3: 0.93%; Cl: 0.01%; La_2O_3: 0.12%; ZrO_2: 0.01%	578	1544, Brönsted
K10	SiO_2: 77.76%; Al_2O_3: 15.6%; Fe_2O_3: 3.10%; MgO: 1.27%; Na_2O: 0.40%; K_2O: 0.78%; CaO: 0.11%; MnO_2: 0.33%; SnO_2: 0.58%; TiO_2: 0.07%[d]	217	1544, Brönsted
KSF	SiO_2: 66.37%; Al_2O_3: 19.73%; Fe_2O_3: 6.46%; MgO: 3.32%; Na_2O: 0.50%; K_2O: 0.93%; CaO: 1.49%; MnO_2: 0.07%; SnO_2: 0.42%; TiO_2: 0.61%; ZrO_2: 0.1%[d]	9	1548, Brönsted
Zr-pillared clay	SiO_2: 17.49%; Al_2O_3: 6.80%; Fe_2O_3: 4.26%; MgO: 0.88%; Na_2O: 0.46%; K_2O: 0.18%; CaO: 0.05%; P_2O_5: 0.12%; TiO_2: 0.70%; ZrO_2: 67.41%; HfO_2: 1.33%	167	[e]

[a] Values obtained by X-ray fluorescence.
[b] Values obtained from N_2 adsorption experiments.
[c] Bands observed by FTIR after pyridine adsorption.
[d] Determined by induced coupled plasma [10].
[e] Not determined.

contact time of 5 ms using ramp shaped pulses on the protons, 2048 scans, a recycle time of 3 s, spinning rates of 8 and 10 kHz and TPPM (with a phase jump of 15°) for proton decoupling. Chemical shifts were measured relative to a H_3PO_4-85% standard and $AlCl_3{\cdot}6H_2O$.

3. Results and discussion

3.1. Alumina

The characterization of the acid sites was done on a sample of γ-Al_2O_3 previously calcined at 823 K for 16 h. The measured BET area (216 m^2/g) was comparable to literature values, between 201 m^2/g [14] and 220 m^2/g [15]. Solid-state ^{27}Al MAS spectrum showed the presence of 18% Al^{IV} at 67 ppm and 82% Al^{VI} 6 ppm (spectrum not shown). The amount of Al^{IV} found in our case is slightly different from previously published results [16,17], which can be ascribed to different synthesis conditions. The acidity evaluation by pyridine adsorption and infrared analysis showed a strong absorption band at 1448 cm^{-1} (Fig. 1, entry I) due to the presence of Lewis sites on the surface of alumina [18]. After desorption at 523 K only a small amount of Lewis adducts was still present, and by increasing the temperature until 623 K no characteristic band was observed anymore, showing that at this temperature the Lewis sites present are not strong enough to interact with pyridine.

Solid-state ^{31}P MAS NMR spectra obtained for γ-Al_2O_3 after calcination to 673 K during 2 h followed by adsorption of 40 Torr TMP at ambient temperature and desorption at this same temperature under vacuum at 2×10^{-5} Torr are illustrated in Fig. 2a.

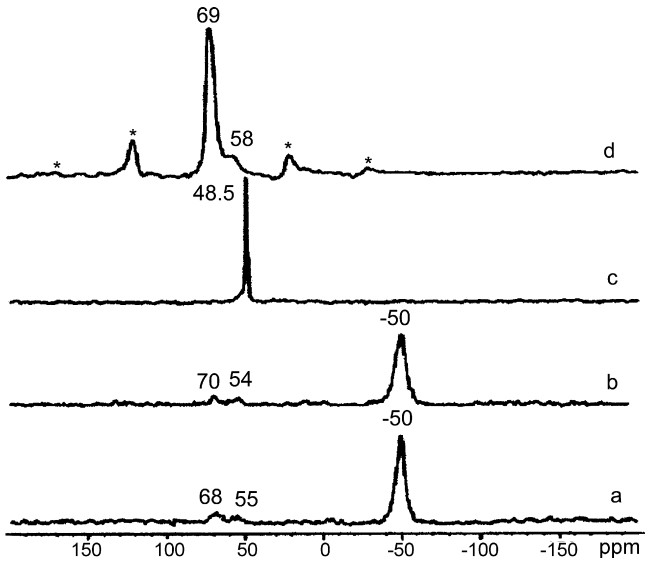

Fig. 2. Solid state ^{31}P-MAS NMR spectra (7.05 Tesla) of γ-Al_2O_3 (a) after adsorption of 40 Torr TMP and vacuum 2×10^{-5} Torr at ambient temperature; (b) after exposure to air for 10 min; (c) after exposure to air for 2 weeks; and (d) submitted to vacuum 2×10^{-5} Torr, at 623 K during 1 h. Asterisks denote spinning sidebands.

An intense signal at −50 ppm is observed, besides two weak signals at 54 and 68 ppm. Liquid TMP resonates at −62 ppm and when physisorbed on the surface of zeolites at −67 ppm [19]; this latter signal was not detected in the spectrum, showing that the desorption procedure was effective. The appearance of small signals with positive chemical shifts indicates that part

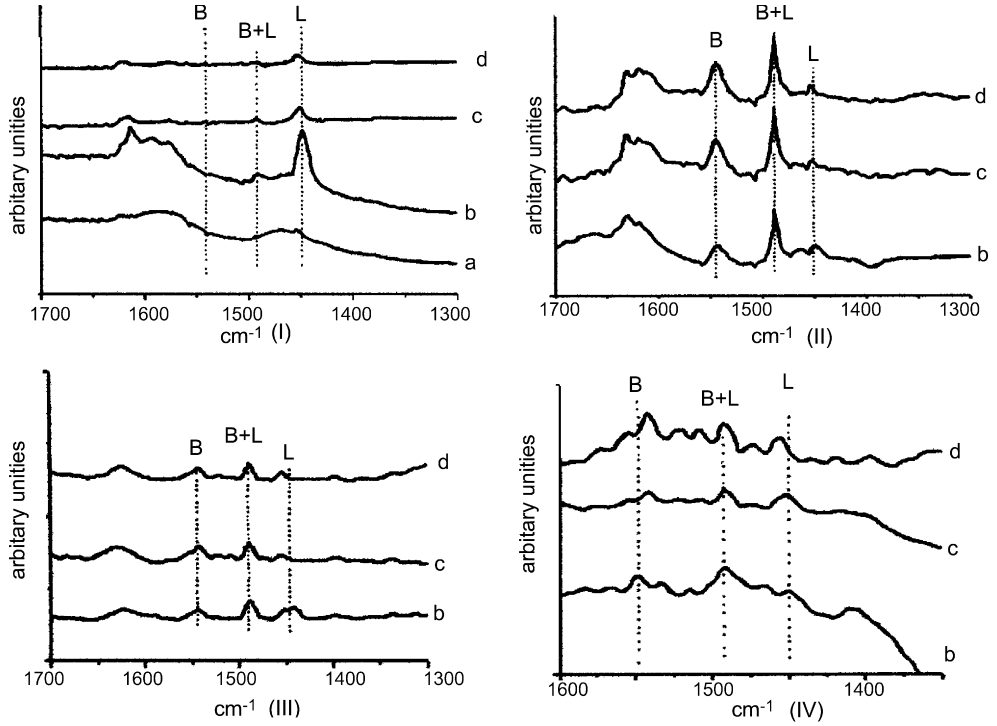

Fig. 1. FTIR spectra of pyridine adsorbed on the surface of acid solids, (I) γ-Al2O3, (II) HY zeolite, (III) K10 clay and (IV) KSF clay: (a) after calcination under vacuum; (b) after adsorption of pyridine and desorption at 423 K; (c) after desorption at 523 K; (d) after desorption at 623 K. B and L denote Brönsted and Lewis adducts respectively.

of TMP was transformed into TMPO during the adsorption step. The sample was then returned to the reactor and a vacuum was applied at 623 K, the same temperature used in FTIR acidity strength evaluation. The signal at −50 ppm disappeared (Fig. 2d) and two new signals were detected, a strong one at 69 ppm presenting first and second order spinning sidebands and a shoulder at 58 ppm. Those spectra can be interpreted on the basis of the data summarized in Table 2, namely a TMP/Lewis adduct for the major peak, in Fig. 2a, with traces of TMPO/Lewis and TMPO/Brönsted sites. These results are in keeping with previous studies, which evidenced the presence of Lewis sites by either using TMP [20–22] or TMPO [23] as a probe. Substantial oxidation products of TMP were observed for substituted [21] or non-functionalized aluminas [20], or otherwise just appeared as trace compounds, like in our case. Heating the sample at 623 K during 1 h under vacuum promotes the oxidation of the TMP, and the subsequent formation of TMPO/alumina adducts, signaled by a peak at 68 ppm. The TMPO is strongly linked to the surface, as suggested by the appreciable chemical shift anisotropy reflected through the large number of spinning sidebands. Guillaume et al. [22] studied the effect of the desorption temperature in γ-Al_2O_3 and chlorinated γ-Al_2O_3 and suggested that strong sites would be the ones maintained above 473 K. They observed the signal at 68 ppm maintained after evacuation at 473 K, in accordance with the results obtained in this work. Fig. 3 summarizes the different species proposed to be present on the surface of γ-Al_2O_3. It should be noted at this point that the IR and the NMR probes demonstrate higher affinity for the acid sites, as no adduct is maintained in the case of pyridine above 673 K. To promote oxidation, the sample was opened to air and NMR spectra recorded after 10 min (Fig. 2b) and 2 weeks (Fig. 2c). The oxidation process, testified by the disappearance of the signal at −50 ppm and the emergence of a new sharp one at 48.5 ppm, is rather slow in these conditions. The observed signal is characteristic of physisorbed TMPO, confirmed by the absence of spinning sidebands and the narrow line width, both indicators of a species weakly linked to the surface of γ-Al_2O_3. It is important to point out that although TMP is easily oxidized by air, TMP to TMPO oxidation has been shown no to be induced during the sample introduction. In the case of the NMR MAS rotors and caps employed here, the part of the sample close to the cap (not detected) is acting as a filter. This is confirmed by the observation that the sample signal does not evolve after exposure to ambient atmosphere by opening the rotor for 10 min (Fig. 2, entry b). Moreover, was also assessed the absence of rehydration of the sample, since the hydration of the alumina surface implies physisorption of TMPO (Fig. 2, entry c), while dehydration leads to chemisorpion of TMPO (Fig. 2, entry d) on the surface of γ-Al_2O_3.

3.2. Zeolite HY

The zeolite HY from FCC process presented BET area of 578 m^2/g after calcination at 776 K during 16 h, somewhat lower compared with the literature, 874 m^2/g from Rakiewicz et al. [14]. The catalyst was characterized by solid-state ^{29}Si MAS NMR, and through the Löwenstein relation the silica/alumina ratio (SAR_{NMR}) was determined as 8.38, which is much higher than measured by X-ray fluorescence (SAR_{XRF} of 2.45, Table 2), evidencing the presence of extra-framework aluminum (EFAl) in this sample. The ^{27}Al MAS NMR spectrum confirmed this result (Fig. 4a), since two signals at 59 ppm (Al^{IV}) from struc-

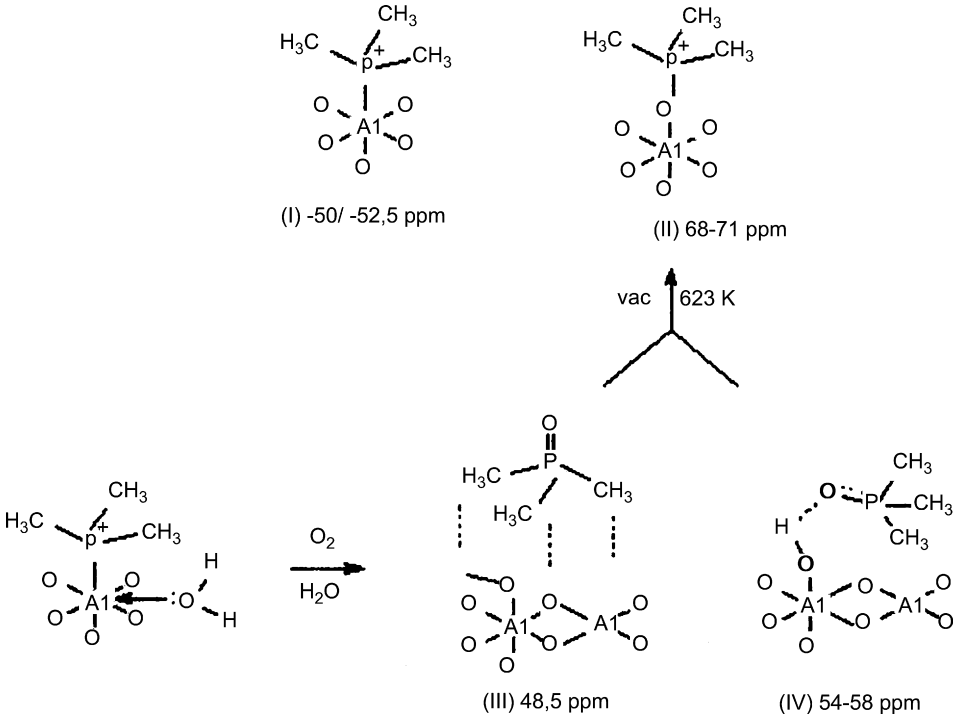

Fig. 3. ^{31}P NMR chemical shifts proposed on the basis of results obtained for γ-Al_2O_3.

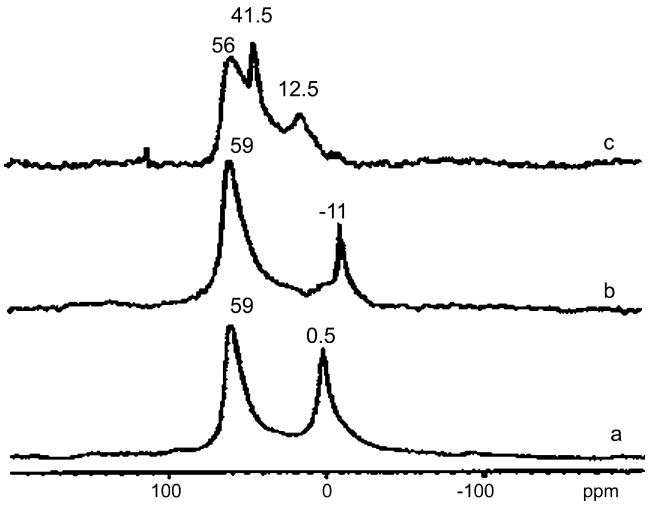

Fig. 4. Solid state ^{27}Al-MAS NMR spectra obtained for HY partially dealuminated: (a) after calcination at 773 K/2 h; (b) after adsorption of TMP followed by desorption under 2×10^{-5} Torr at ambient temperature; and (c) after desorption 2×10^{-5} Torr under 623 K during 1 h.

tural aluminum and at 0.5 ppm (Al^{VI}) from extra-framework aluminum were observed, similar to what reported by Kao et al. [25]. EFAl species are generated during the preparation of the acid form of the catalyst, and can be extracted by hot water and $(NH_4)_2SO_4$ [14] or with diluted H_2SO_4 [26], but in our case we kept the catalyst in its working form. Two types of EFAl species have been proposed in the literature: cationic particles like Al^{3+}, AlO^+, $Al(OH)^{2+}$, and $Al(OH)_2^+$, and neutral or polymeric aluminum species, e.g., AlO(OH), $Al(OH)_3$, and Al_2O_3 [25]. The characterization of acid sites by FTIR with pyridine (Fig. 1, entry II) shows a strong absorption at 1544 cm^{-1}, due to Brönsted sites and a small absorption at 1451 cm^{-1}, due to Lewis sites present in EFAl species already detected by ^{27}Al MAS NMR. The acid strength was estimated after pyridine desorption at 523 and 623 K and showed that strong Brönsted sites are present, since the band persists after treatment.

3.3. Evolution of the structure through aluminum NMR

The acidity evaluation by NMR was done after calcination of HY at 673 K during 2 h followed by adsorption of TMP at ambient temperature and evacuation. We first discuss the evolution of the material due to the NMR protocol. The ^{27}Al MAS NMR spectrum (Fig. 4b) showed that the signal due to structural aluminum does not change after exposure to TMP, but almost all the signal observed at 0.5 ppm (extra-framework Al^{VI} sites) vanishes and a new signal at −11 ppm appeared, indicating that basic phosphine molecules reacted with these sites. The chemical shift is in the same region observed for octahedral aluminum sites similar to Al^{VI}–O–P in hydrated AlPOs, located at −15 ppm [27,28]. We therefore suggest that the phosphine is adsorbed on EFAl of the type $Al(OH)_2^+$ [29], with subsequent reaction to form Al^{VI}–O–P linkages. After calcination at 623 K during 1 h under vacuum (Fig. 4c) the signal at −11 ppm disappeared and two new signals appeared at 12.5 and 41.5 ppm. This evolution can be explained if the calcination process would lead to dehydroxylation of the Al^{VI}–O–P sites already present, with the formation of Al^{V}–O–P and Al^{IV}–O–P species. The signal at 41.5 ppm is very narrow, which implies symmetry or mobility. By analogy with the chemical shift observed for dehydroxylated AlPOs [27,28] at 38 ppm (Al^{IV}–O–P sites) we suggest that the signal at 41.5 ppm is due to $Al^{IV}[OP(CH_3)_3]_4$ species, and its lower symmetry homologue, $Al^{V}(OH)[OP(CH_3)_3]_4$ is responsbile for the broader peak at 12.5 ppm. To the best of our knowledge it was the first time that ^{27}Al MAS is reported for phosphine adsorbed on EFAl in HY zeolite.

3.4. Acid sites

Fig. 5a shows the ^{31}P MAS NMR spectrum obtained for HY after adsorption of TMP and desorption at ambient temperature under vacuum. Signals were detected at −2 ppm and at 25, 44, 56, 64 and 79 ppm, without appreciable changes even after storing the sample for 1 month (Fig. 5b). Again, the signal at −67 ppm due to physisorbed TMP was not observed.

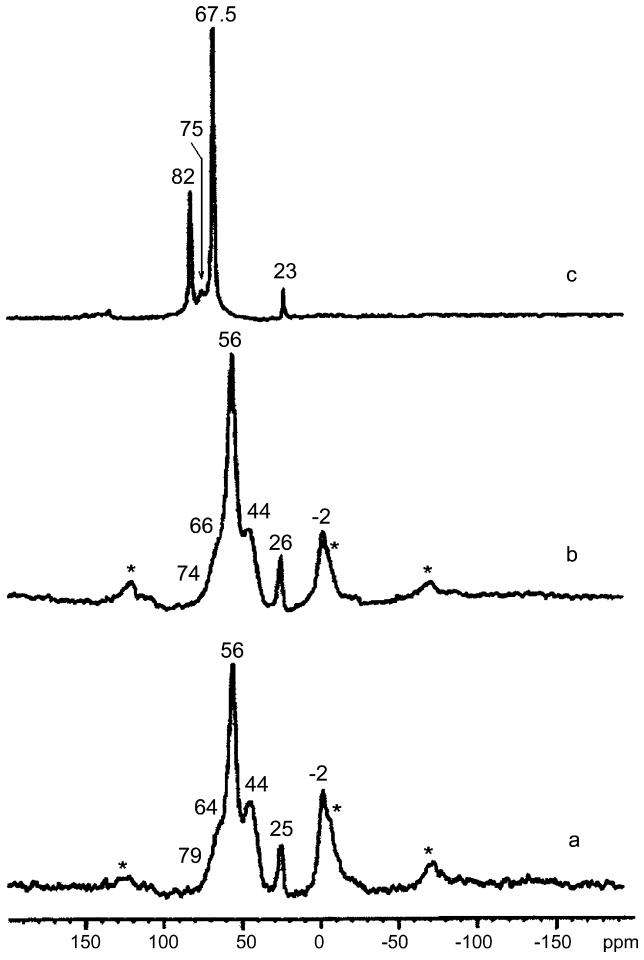

Fig. 5. Solid state ^{31}P-MAS NMR spectra (7.05 Tesla) obtained for partially dealuminated HY zeolite: (a) after adsorption of TMP followed by vacuum at 2×10^{-5} Torr at ambient temperature; (b) after 2 months storage inside a glove bag; and (c) after being under vacuum (2×10^{-5} Torr) at 623 K during 1 h. Asterisks denote spinning sidebands.

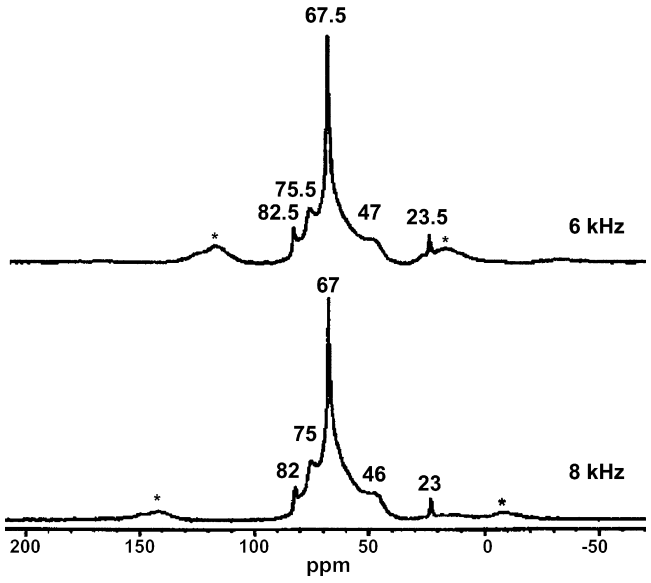

Fig. 6. Solid state ^{31}P-CPMAS spectra (9.4 Tesla) obtained for zeolite HY at distinct spinning rates. Asterisks denote spinning sidebands.

After high-temperature desorption (Fig. 5c) a rather puzzling feature appears, namely the presence of narrow signals, which in the context of solid-state NMR are usually indicative of labile or mobile species. To gain further knowledge on the nature of the adducts after desorption at high temperature, we submitted this sample to a proton-to-phosporus cross-polarization experiment. This procedure enhances the signal intensities of immobilized species. Fig. 6 shows that, in fact, the narrow signals in this experiment become relatively less important. Moreover, it becomes apparent the presence of spinning sidebands, associated with a broad peak, located right beneath the narrow signal at 67 ppm. Extensive work on the characterization of zeolites by phosphorus-containing NMR probes has been the object of recent work and most of our signals are in line with these results. The peak at about −2 ppm can be assigned to TMP in contact with Brönsted sites (Table 1), most of the other peaks being assignable to TMPO species. This latter molecule has a higher sensitivity towards Brönsted acidity, as it is able to react differently to the several sites present in a zeolite, with signals in the region between 65 and 90 ppm. This variability of the resonance assigned to Brönsted site-TMPO adducts has been explained invoking the variation of the amount of localization of the acid proton on the TMPO side. The adduct bond between phosphine oxide and Bronsted sites can be interpreted in terms of frontier orbitals [30], with the overlap of the HOMO of the oxygen and the LUMO of the hydrogen in the acid site; as the electron density around phosphorous is consequently lowered, its chemical shift will displace to higher frequencies. In other words, a direct relation between the phosphorus chemical shift of the probe and the acid strength of the site should be found. Zeolites with the faujasite structure present four crystallographic positions that can be occupied by Brönsted acid sites, named O_1–O_4. Ward and Hansford [31] concluded by IR experiments that the site O_4 in HY was not occupied by acid hydrogens, and the occupation ratio $O_2 + O_3/O_1$ was 0.9/1. Analysis of NMR spectra of TMPO adsorbed on zeolite HY [8] evidenced two peaks at 55 and 65 ppm, corresponding to sites with different acid strength. The first of the pair is the most accessible and labile one, confirmed by our desorption experiments (Figs. 5c and 6). It can be assigned to an oxygen site in the supercage, consistently with previous work. The second signal, at 65 ppm, is more persistent, as it can be still detected after desorption in the cross-polarization experiment, so that it can be assigned to a site in the sodalite cage.

The presence of a peak at about 44 ppm is usually attributed to physisorbed TMPO. However, Figs. 5a and 6 demonstrate the persistence of the associated species after desorption at high temperature. We should deduce that the zeolite used here presents sites where non-protonated TMPO molecules can be strongly held. The other peaks listed in Fig. 5a–c have never been observed before in zeolite HY.

A signal observed in the range 23–27 ppm was detected by various researchers in other materials [19,20,32,33] but its assignment was not clear until Haw et al. [34], studying the adsorption of TMP on sulfated zirconia catalysts by NMR and theoretical calculations, unveiled its provenance to $[(CH_3)_4P]^+$ species, generated from reaction between TMP and the $[TMP\text{-}H]^+$ adduct. Shimizu et al. [35] suggested that the formation of $[(CH_3)_4P]^+$ is an indication of the presence of strong Brönsted acid sites. In our analysis, this signal persists after high-temperature desorption, which testifies a strong interaction of the phospho-cation with the solid, probably with an oxygen, which has completely given up its hydrogen. The presence of this signal can thus, be used to infer strong Brönsted sites. After calcination at 623 K during 1 h under vacuum, the signals at −2, 44 and 56 ppm disappeared (Fig. 5c); the signals at 23, 67.5 and 75 ppm persisted, the first two with narrower line widths, compared to the spectrum in Fig. 5b. A new signal appeared at 82 ppm. The presence of narrow signals after desorption at 673 K is rather puzzling, as it indicates concurrent molecular mobility and strong bonds to the inorganic solid of the organic probe. On the basis of the evolution of the aluminum spectrum discussed above, and more specifically the EFAl part, we propose that the narrow signals correspond to TMPO:Al_{EFAl} adducts, with tetra- and penta-coordinated aluminum.

The analysis of the NMR spectra demonstrate that in this zeolite most of the TMP is readily oxidized to TMPO. The chemical analysis evidenced the presence of 0.93% of SO_3, which is possibly the oxidative species responsible for the large amount of oxidation of TMP to TMPO. The surviving TMP molecules are all in coordination with Brösted sites, consistently with the low calcination temperature used in this study.

It should be noted that the results presented here for a catalyst from the plant present some differences with previous studies of zeolite HY, most notably concerning non-structural sites. Interestingly, this result points toward different acid characteristics between a working catalyst and a model one. Further experiments are in progress in order to correlate in a quantitative sense the sharp signals observed here for the first time with the acid sites present in HY zeolite.

3.5. Clays

The ^{27}Al MAS spectrum of the K10 clay presented signals in the range 60–68 ppm (two different Al^{IV} sites) and at 4 ppm (Al^{VI} sites). The same was observed for the KSF clay [36]. The spectrum of the Zr-pillared clay presented a very intense signal at around 4 ppm (Al^{VI} sites) and a small signal in the region of the Al^{IV} sites. The ^{27}Al MAS spectrum of K10 after a cycle of adsorption/desorption of TMP remains very similar (spectra not shown). The absence of signals in the negative region of the spectrum indicates that non-structured aluminum sites, usually generated during the synthesis due to acid treatment, are absent in this material.

The evaluation of acidity by pyridine showed only weak IR bands due to Brönsted sites, for K10 (Fig. 1, entry III) on 1544 cm^{-1}, while for KSF (Fig. 1, entry IV) a band at the literature value of 1548 cm^{-1} can be only guessed, due to poor signal-to-noise ratio [37]. In the ^{31}P MAS NMR spectrum of K10 clay after adsorption of TMP (Fig. 7a) it was observed an intense signal at −6 ppm, due to $[TMP\text{-}H]^+$ adduct, and signals at 45, 64 and 80 ppm, corresponding to physisorbed molecules and $[TMPO\text{-}H]^+$ adducts. After desorption at 623 K (Fig. 7b) the signal at −6 ppm disappeared, and only the signals in the positive region of the spectrum could be observed, at 68 and 80 ppm, revealing the presence of strong Brönsted sites, if we accept the validity of Table 1 for the case of clays. The oxidation of TMP to TMPO in this clay was promoted probably by Fe^{3+}, together with structural water. Similar results were obtained for the KSF clay (Fig. 8a and b) and also for the Zr-pillared clay (Fig. 9a and b). The large number of spinning sidebands observed here is due to the chemical shift anisotropy induced by the proximity of structural Fe^{3+}, which is more abundant in these samples compared to K10 (Table 2). Even in such condition of reduced resolution, we could clearly see a signal at 4 ppm (KSF) and −8 ppm (Zr-pillared clay) after adsorption of TMP. Desorption at 623 K induce the evolution of the spectra, in which the signals observed for those clays are in the range 85–58 ppm, due to a

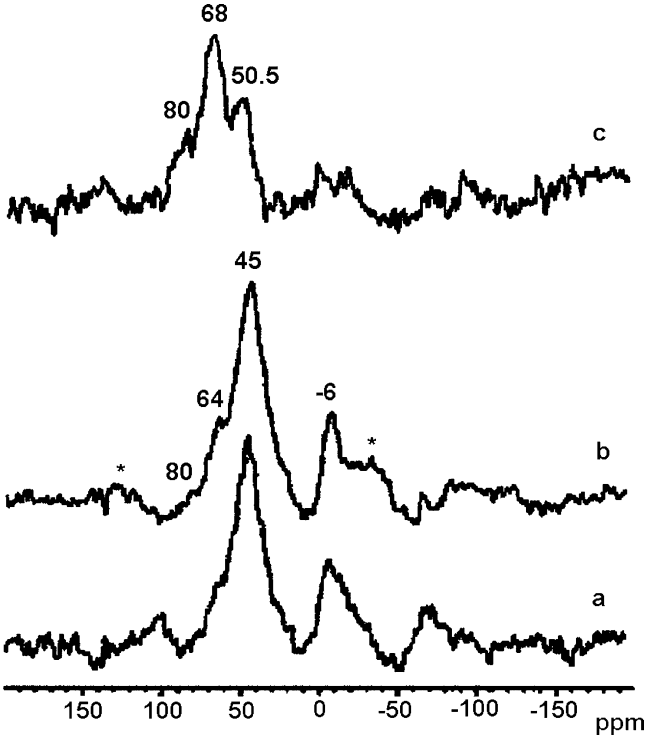

Fig. 7. Solid state ^{31}P-MAS NMR spectra obtained for K10 clay: (a) after adsorption of TMP and vacuum 2×10^{-5} Torr, 6 kHz spinning speed; (b) same as (a), but at 8 KHz spinning speed; and (c) after being under vacuum (2×10^{-5} Torr) at 623 K during 1 h.

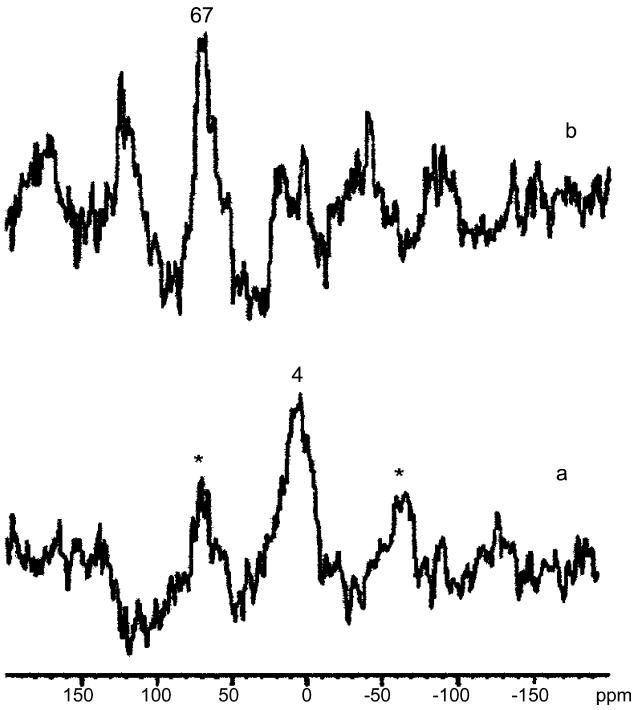

Fig. 8. Solid state ^{31}P-MAS NMR spectra obtained for KSF clay: (a) after adsorption of TMP and desorption 2×10^{-5} Torr at ambient temperature; and (b) after dessorption 2×10^{-5} Torr at 623 K during 1 h.

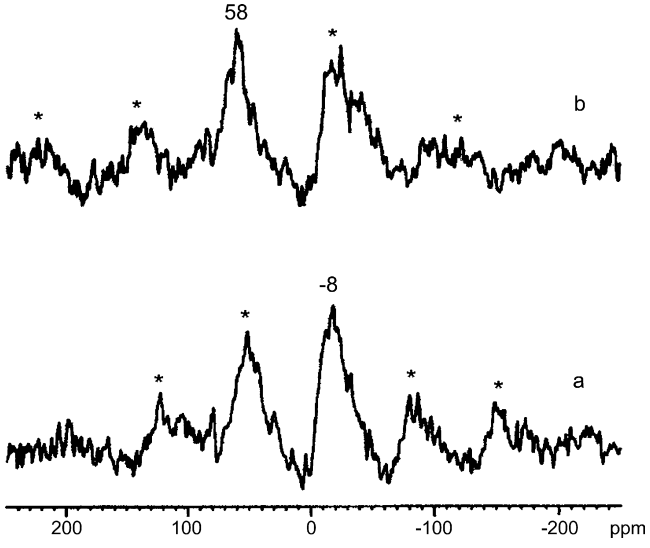

Fig. 9. Solid state ^{31}P-MAS NMR spectra obtained for Zr-pillared clay: (a) after adsorption of TMP at ambient temperature; and (b) after dessorption 2×10^{-5} Torr at 623 K during 1 h.

$[TMPO-H]^+$ adduct. Oxidation on this material thus, requires a temperature activation, the high iron concentration notwithstanding. The difference in the spectra of the three clays would indicate that K10 has a larger acid site number and acid site strength distribution than KSF and Zr-pillared clay, consistently with the difference in surface area. However, the low resolution of the KSF and Zr-pillared clay spectra precludes any quantitative consideration at this point. Further studies are in progress in order to increase the quality of the spectra and to quantify the acid sites present by using spin counting experiments, to compare our results with the ones published by Hart and Brown [10] for K10 acidity determination by using ammonia adsorption microcalorimetry.

4. Conclusions

We have shown that TMP is an excellent NMR probe of redox properties for actual working acidic catalysts. The nature of the acid sites present in K10, KSF and Zr-pillared clays were also investigated here for the first time by using TMP as a probe, and compared with those present in γ-Al_2O_3 and HY zeolite containing extra-framework aluminum by ^{31}P and ^{27}Al solid-state NMR. It was found that metal impurities are a factor, but not the only one, in the oxidation of TMP to TMPO. Al^{IV}–O–P, Al^{V}–O–P and Al^{VI}–O–P extra-framework species were proposed to play a special role in the sample of HY after adsorption of TMP, on the basis of the evolution of the solid-state ^{27}Al MAS. The system and the methodology applied here were shown to be appropriate for the characterization of Lewis and Brönsted acid sites present in the catalysts studied, which were actual specimen used in the synthesis or industrial plants.

Acknowledgements

Donations of γ-Al_2O_3 (Dr. Maria Auxiliadora S. Baldanza, UFRJ) and HY (Prof. José Luiz Monteiro, UFRJ) are gratefully acknowledged. The authors thank Deborah C. Vargas (UFRJ) for IR measurements. The financial support of the CAPES-COFECUB-Program 436/03 is also acknowledged.

References

[1] W.E. Farneth, R.J. Gorte, Chem. Rev. 95 (1995) 615.
[2] W.H. Chen, T.C. Tsai, S.J. Jong, Q. Zhao, C.T. Tsai, I. Wang, H.K. Lee, S.B. Liu, J. Mol. Catal. A: Chem. 181 (2002) 41.
[3] S.J. Huang, Q. Zhao, W.H. Chen, X. Han, X. Bao, P.S. Lo, H.K. Lee, S.B. Liu, Catal. Today 97 (2004) 25.
[4] S.J. Huang, Y.H. Tseng, Y. Mou, S.B. Liu, S.H. Huang, C.P. Lin, J.C.C. Chan, Solid State Nucl. Magn. Reson. 29 (2006) 225.
[5] P.J. Chupas, C.P. Grey, J. Catal. 224 (2004) 69.
[6] J. Zhuang, D. Ma, Z. Yan, F. Deng, X. Liu, X. Han, X. Bao, X.W. Liu, X. Guo, X. Wang, J. Catal. 221 (2004) 670.
[7] D.J. Zalewski, P. Chu, P.N. Tutunjian, J.H. Lunsford, Langmuir 5 (1989) 1026.
[8] M.D. Karra, PhD Thesis, Pennsylvania State University, 2002.
[9] V. Mavrodinova, M. Popova, R.M. Mihályi, G. Pál-Borbély, C. Minchev, Appl. Catal. A 248 (2003) 197.
[10] M.P. Hart, D.R. Brown, J. Mol. Catal. A: Chem. 212 (2004) 315.
[11] G. Nagendrappa, Resonance 7 (2002) 64.
[12] A.W.S. Guarino, S.M.C. Menezes, L.C. Dieguez, R.A.S. San Gil, Proceedings of the EUROPACAT III, Krakow, 1997, p. 289.
[13] J.A. van Khoven, D.C. Koningsberger, P. Kunkeler, H. van Bekkum, A.P. Kentgens, J. Am. Chem. Soc. 122 (2000) 12842.
[14] E.F. Rakiewicz, A.W. Peters, R.F. Wormsbecher, K.J. Sutovich, K.T. Mueller, J. Phys. Chem. B 102 (1998) 2890.
[15] B.A. Huggins, P.D. Ellis, J. Am. Chem. Soc. 114 (1992) 2098.
[16] H.D. Morris, P.D. Ellis, J. Am. Chem. Soc. 111 (1989) 6045.
[17] M.H. Lee, C.F. Cheng, V. Heine, J. Klinowski, Chem. Phys. Lett. 265 (1997) 673.
[18] M. Niwa, N. Katada, Y. Murakami, J. Phys. Chem. 94 (1990) 6441.
[19] W.P. Rothwell, W.X. Shen, J.H. Lunsford, J. Am. Chem. Soc. 106 (1984) 2452.
[20] J.H. Lunsford, W.P. Rothwell, W. Shen, J. Am. Chem. Soc. 107 (1985) 1540.
[21] T.C. Sheng, I.D. Gay, J. Catal. 145 (1994) 10.
[22] D. Guillaume, S. Gautier, I. Despujol, F. Alario, P. Beccat, Catal. Lett. 43 (1997) 213.
[23] L. Baltusis, J. Frye, G.E. Maciel, J. Am. Chem. Soc. 108 (1986) 7119.
[24] W. Hu, Q. Luo, Y. Su, L. Chen, Y. Yue, C. Ye, F. Deng, Micropor. Mesopor. Mater. 92 (2006) 22.
[25] H.M. Kao, C.Y. Yu, M.C. Yeh, Micropor. Mesopor. Mater. 53 (2002) 1.
[26] S.M.C. Menezes, V.L. Camorim, Y.L. Lam, R.A.S. San Gil, A. Bailly, J.P. Amoureux, Appl. Catal. A 207 (2001) 367.
[27] S. Caldarelli, A. Meden, A. Tuel, J. Phys. Chem. B 103 (1999) 5477.
[28] A. Tuel, S. Caldarelli, A. Meden, L.B. McCusker, C. Baerlocher, A. Ristie, N. Rajic, G. Mali, V. Kaucie, J. Phys. Chem. B 104 (2000) 5607.
[29] H.M. Kao, Y.C. Chen, C.C. Ting, P.T. Chen, J.C. Jiang, Catal. Today 97 (2004) 13.
[30] J.P. Osegovic, S. Drago, J. Phys. Chem. B 104 (2000) 147.
[31] J.W. Ward, R.C. Hansford, J. Catal. 13 (1969) 364.
[32] D.J. Coster, A. Bendada, F.R. Chen, J.J. Fripiat, J. Catal. 140 (1993) 497.
[33] J.H. Lunsford, H. Sang, S.M. Campbell, C.H. Liang, R.G. Anthony, Catal. Lett. 27 (1994) 259.
[34] J.F. Haw, J. Zhang, K. Shimizu, T.N. Venkatraman, D.P. Luigi, W. Song, D. Barich, J.B. Nicholas, J. Am. Chem. Soc. 122 (2000) 12561.
[35] K. Shimizu, T.N. Venkatraman, W. Song, Appl. Catal. A 224 (2002) 77.
[36] T. Cseri, S. Bekassy, F. Figueras, E. Csere, L.C. Menorval, R. Dutartre, Appl. Catal. A 132 (1995) 155.
[37] F. Figueras, T. Cseri, S. Bekassy, E. Csere, L. Menorval, R. Dutartre, Appl. Catal. A 132 (1995) 141.